

EXPERIMENTAL OBSERVATION OF STABILIZATION OF TIPPE TOP SPINNING ON A VIBRATING PLANE

Alexander A. Kilin and Yury L. Karavaev

ABSTRACT. This paper presents an experimental study of the motion of a spherical body with a displaced center of mass on a surface undergoing oscillations in the vertical plane. The phenomenon of vibrostabilization of an unstable position in which the center of mass of the body is above the geometric center of the sphere is revealed. The influence of the frequency and amplitude of oscillations of the surface on the stabilization of the unstable position of the motion of the spherical body is analyzed.

1. Introduction

A spherical top (or a tippe top) is an interesting and illustrative example of a rigid body that exhibits dynamical behavior. To date, there has been a large body of research on this topic [1–10]. These studies discuss the problems of describing the motion and explaining the inversion of the top, investigate the stability of its motion, including the influence of the parameters of a rigid body on stability, and describe the forces of contact interaction and their influence on the behavior of a dynamical system.

The results of the above investigations can be applied to describe the motion and control of more complex mechanical systems such as spherical mobile robots [11–16]. The review papers [15, 16] demonstrate a wide variety of designs of spherical robots and conditions of their application, including the motion on a surface undergoing oscillations [20–23]. These papers present theoretical investigations of the stability of the motion of spherical robots and methods of stabilizing their motion on a surface undergoing oscillations. This will make it possible to expand the scope of application of spherical robots and to ensure the precision of their motion. However, due to the complexity of the mechanical system the results obtained are theoretical in nature and have not yet been validated in practice. Moreover, in investigating such systems, one often considers simpler mechanical models.

2020 *Mathematics Subject Classification:* 74H45; 70-05, 70E50.

Key words and phrases: spherical top, vibrating plane, stabilization, experiment.

For example, in the papers [17–19] published recently, a great deal of attention is given to the problem of stabilizing a spherical top or an ellipsoid of revolution with a displaced center of mass during its motion on a plane undergoing oscillations, which is used as a simplified model of a spherical robot.

The use of fast oscillations for stabilization of mechanical systems, particularly in theoretical treatments, was initiated in Refs. [24–28] devoted to the stabilization of a one-degree-of-freedom inverted pendulum by means of fast oscillations of its suspension point. These studies served as a basis for a new field of engineering—vibration engineering [29] (also called *vibration mechanics* [30]).

The development of the theory of analysis of pendulum systems with a vibrating suspension point is discussed in Refs. [33–38], in which the dynamics of the systems and the conditions for their stability are investigated. In [52, 53], the dynamics of the motion of a rattleback on a surface undergoing oscillations is examined. Bifurcation diagrams are constructed and periodic solutions of the system are investigated. The possibility of using such a mechanical system as an energy harvesting system is considered.

The hypotheses of the possibility of the motion of spherical and wheeled mobile robots by means of small periodic control actions are based on the results of investigating the problem of maintaining constant speedup of a wheeled vehicle by periodically changing the mass distribution [39, 40] and the problem of speeding up the Chaplygin top by means of an internal rotor [41]. Furthermore, the development of vibrational propulsion devices of mobile robotic systems and the motion performed by means of oscillations of internal mechanisms [32, 42–51] is studied. The complexity of the behavior of systems with friction in the presence of vibrations is discussed in [54]. The efficiency of the control of mechanical systems undergoing forced oscillations is demonstrated in publications on the control of resonant manipulation robots [55] and other technical systems and applications [31, 56].

The aim of this paper is to experimentally estimate the possibility of using vibrations for stabilization of a spinning tippe top when its center of mass is in the upper unstable position and to compare the results obtained with those of theoretical investigations presented in [19].

2. Description of the experimental facility and the object of research

To carry out experimental investigations for estimating the stabilization of the spinning top by means of vertical oscillations of the base, a using a specially developed test bench: a vibrating table. Parts a and b of Fig. 1 show, respectively, a three-dimensional model and a photograph of this experimental facility. The table board (in the form of a horizontal plane) is mounted on spring supports and is actuated by eccentrics rotated by direct current motors through a belt drive. The magnitude of eccentricity determines the oscillation amplitude of the table, and the voltage that is fed to the direct current motor determines the angular velocity of the eccentrics, i.e., the frequency of vibrations. Vertical guides ensure that the table board moves only in the vertical plane. The design shown in Fig. 1b makes it possible to change the oscillation amplitude δ from 0 to 2.5 mm for a range of oscillation frequencies of the surface f from 0 to 7 Hz.

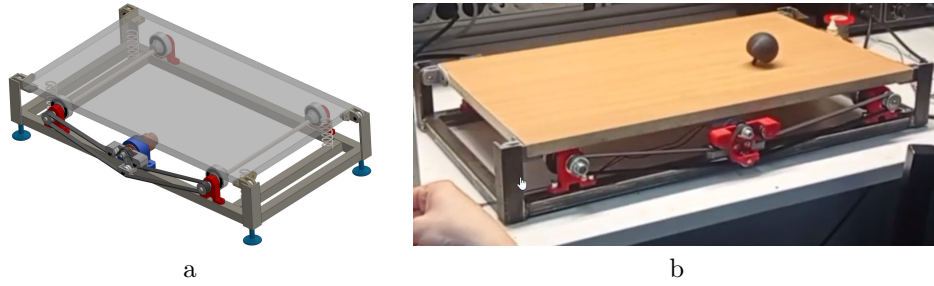


FIGURE 1. Experimental facility: a-3D model of a test bench for generation of oscillations, b-photograph of the laboratory facility.

An optical camera was mounted above the test bench to experimentally determine the spin rate ω of the top by measuring the change in the angular position of the special marker.

The spherical top was 3D printed using PET plastic. The top starts spinning and reaches a sufficient spin rate owing to the fact that it has a narrow cylindrical stem on which spinning occurs after the top flips over (see Fig. 2). The top was spun by hand, but the capture of motion began at the instant when the top flipped over and the optical system identified the marker drawn on its surface (see Fig. 3). The spherical top is a truncated sphere with a cylindrical narrow stem fastened to it. The end of the stem is a spherical segment (of smaller radius). The parameters of the experimental top are denoted by symbols with a hat ($\hat{\cdot}$) above them:

- the mass of the top $\hat{m} = 13.6$ g;
- the axial moments of inertia $\hat{i}_1 = \hat{i}_2 = 3232$ g \cdot mm², $\hat{i}_3 = 3145$ g \cdot mm²;
- the displacement of the center of mass relative to the center of the truncated sphere: $\hat{a} = 7$ mm;
- the radius of the spherical body of which the top is made: $\hat{R} = 22.5$ mm;
- the height of the top $\hat{h} = 43$ mm;
- the radius of curvature of the surface of the top's stem on which the top spins $\hat{\rho} = 7$ mm.

To analyze the stability of vertical rotations, we will use a mathematical model of the top in the form of an ellipsoid proposed in [19]. To ensure that the ellipsoid model provides a correct description of the rotation of the top near the vertical rotations, we require that the parameters of the ellipsoid satisfy the following conditions:

- The mass of the ellipsoid is the same as that of the top: $m = \hat{m} = 13.6$ g.
- The axial moments of inertia of the ellipsoid and the top are the same: $i_1 = i_2 = \hat{i}_1 = \hat{i}_2 = 3232$ g \cdot mm², $i_3 = \hat{i}_3 = 3145$ g \cdot mm².
- For the upper position of the center of mass, the heights of the spherical top and the ellipsoid are the same: $h = \hat{h}$.
- The heights of the centers of mass in the upper position of the spherical top and the ellipsoid are the same: $r = \hat{r} = \hat{h} - \hat{R} + \hat{a}$.

- The radius of curvature of the surface of the spherical top and that of the ellipsoid at the point of contact with the plane are the same: $\rho = \hat{\rho}$. For the case considered here, $\hat{\rho}$ is the radius of curvature of the cylindrical stem on which the top spins.

With these conditions in mind, the geometric parameters of an equivalent ellipsoid (see Fig. 2) with semiaxes $b_1 = b_2$ and b_3 are determined as follows:

$$b_3 = \hat{h}/2, \quad b_1 = b_2 = \sqrt{\hat{\rho} \cdot b_3}, \quad a = \hat{a} + \hat{h} - \hat{R} - b_3,$$

and their values, which were used later, are given by

$$b_3 = 21.5 \text{ mm}, \quad b_1 = b_2 = 12.27 \text{ mm}, \quad a = 6 \text{ mm}.$$

In [19], the condition for stability of the spinning of the top in the upper position of the center of mass is formulated for an ellipsoid in the form of an inequality for the projection of the dimensionless angular momentum of the top onto the axis of its rotation $c = \frac{i_3 \omega}{mb_3^2} \sqrt{\frac{b_3}{g}}$, where ω is the spin rate of the top and g is the free-fall acceleration:

$$(2.1) \quad c^2 > c_*^2 = c_0^2 - \frac{4\nu^2(\lambda - \beta^2)^2}{(\nu + \eta\beta^2\lambda)^2} \Theta^2,$$

where $\nu = \frac{i_3}{i_1}$, $\beta = \frac{b_1}{b_3}$, $\eta = \frac{mb_3^2}{i_1}$, $\Theta^2 = \frac{2\delta^2 \pi^2 f^2}{b_3 g}$, $\alpha = \frac{a}{b_3}$, $\lambda = 1 + \alpha$, and the critical value of the projection of the angular momentum c_0 onto the symmetry axis of the top in the absence of vibrations is defined as

$$c_0^2 = \frac{4\nu^2(1 + \eta\lambda^2)(\lambda - \beta^2)}{\eta(\nu + \eta\beta^2\lambda)^2}.$$

A graphical representation of the dependence of the critical spin rate, at which the upper position of the top loses stability, on the values of the amplitude and

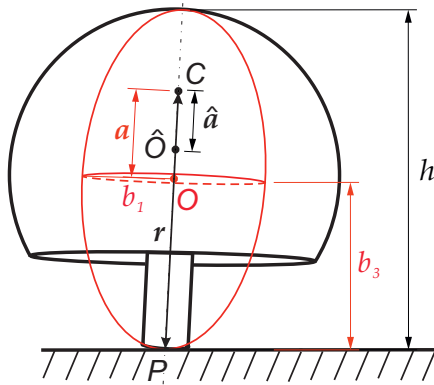


FIGURE 2. Diagram of replacement of the top by an ellipsoid with a displaced center of mass



FIGURE 3. Individual frame with an optical image capture system demonstrating the motion of the top in the inverted position

frequency of oscillations of the surface on which the top moves is shown in Fig. 4 with the technical limitations of the oscillation parameters of the table taken into account.

For the mass-inertia parameters of the top which correspond to the developed prototype, the critical spin rate changes from the value 66.69 s^{-1} , at which there are no vibrations, to the value 64.98 s^{-1} corresponding to the oscillation amplitude $\delta = 2.5 \text{ mm}$, and the oscillation frequency $f = 7 \text{ Hz}$. In theory, an increase in the frequency and amplitude of oscillations of the table leads to a decrease in the critical spin rate of the top, i.e., the spinning of the top becomes longer.

In the experiments, the spin rate of the top was determined from discrete frame images obtained with a frequency of 60 Hz . The top was spun on the table's surface by hand with an initial velocity sufficient for the top's inversion in the first seconds of motion. After the inversion, the table began to vibrate, and the process of image video capture started, which was used later to experimentally determine the spin rate of the top. Next, using the video capture system, the instant of the fall of the top and the critical spin rate, at which the loss of stability of the upper position occurs, were determined.

Figure 5 shows graphs of the spin rates of the top on a fixed base versus time, which correspond to five experiments. The marker "o" in the graphs of the spin rates indicates the initial values obtained at the instant of the top's inversion, and the marker "x" indicates the values at which the top falls over. For clarity and ease of comparison (especially of the terminal motion), the graphs were adjusted so that the initial spin rate of the top in each experiment lay on the curve obtained for the experiment with the maximal initial spin rate. It can be seen from the figure that, despite different initial conditions (the top was set spinning by hand), the changes in the spin rate during motion are the same for all the five experiments. The average value of the spin rate at which the body comes to a stop, in the five

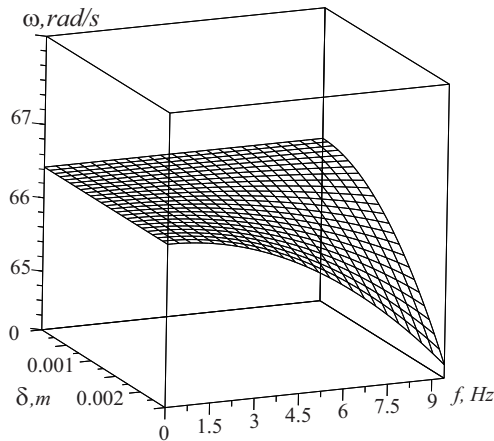


FIGURE 4. Dependence of the critical spin rate of the top on the oscillation parameters of the table's surface

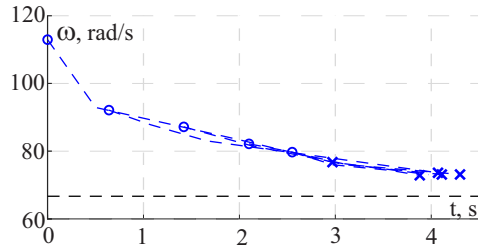


FIGURE 5. Time dependences of the spin rates of the body on a fixed base, for different initial spin rates

experiments carried out independently, was $\hat{\omega} = 73.17 \pm 0.34$ rad/sec. Here and in what follows, the confidence interval for average values was calculated by using t -distribution with a probability of 95%.

The resulting experimental value differs greatly from the value $\omega = 66.69$ rad/sec (shown as a dashed line in Fig. 5) obtained using the criterion (2.1). However, it should be noted that, in practice, quite a number of factors preclude ideal experimental conditions, for example, manufacturing errors, measurements of the spin rate, deviation of the surface from the horizontal line, etc.

In Section 3, the results of application of this experimental facility and methods for comparative estimation of the critical spin rates for different surface oscillation parameters in the vertical plane will be considered.

3. Results of experimental investigations

Figure 6 shows graphs of the spin rates of the body on a vibrating base with an amplitude of 0.5 mm. The graph of the spin rate with the base fixed is shown in black as a reference dependence. For each frequency, a series of five experiments were carried out. Typical graphs of the spin rates of the body versus time are shown in green for a surface oscillation frequency of 3 Hz, in red for 5 Hz, and in blue for a base oscillation frequency of 7 Hz. The markers “o” and “x” in the graphs of spin rates show the initial values and the values before the fall of the top, respectively.

Despite different initial spin rates, the loss of stability of the body (fall) occurs on average at $\hat{\omega} = 70.94 \pm 0.84$ rad/sec for a surface oscillation frequency of 3 Hz (in theory $\omega = 66.68$ rad/sec), $\hat{\omega} = 67.86 \pm 1.1$ rad/sec for a surface oscillation frequency of 5 Hz (in theory $\omega = 66.65$ rad/sec), and $\hat{\omega} = 63.58 \pm 0.82$ rad/sec at 7 Hz ($\omega = 66.62$ rad/sec). That is to say, one can observe a decrease in the spin rate at which a fall occurs, as the frequency of oscillations of the base increases. In the experiment, this tendency is more pronounced. Such dependences have been obtained for large oscillation amplitudes.

Figure 7 shows graphs of the spin rates of the body on a vibrating base with an amplitude of 2.5 mm. As before, black indicates as a reference dependence, a graph of the spin rate with the base fixed. Blue indicates graphs of the spin rate of the body at a surface oscillation frequency of 7 Hz, red indicates graphs of the spin rate of the body at a surface oscillation frequency of 5 Hz, and green at 3 Hz.

In these experiments, the body flips over from the upper unstable position at a surface oscillation frequency of 7 Hz when the average spin rate is $\hat{\omega} = 62.48 \pm 0.59$ rad/sec ($\omega = 64.97$ rad/sec), at 5 Hz when $\hat{\omega} = 65.85 \pm 0.53$ rad/sec ($\omega = 65.82$ rad/sec), and at 3 Hz, when $\hat{\omega} = 70.21 \pm 1.62$ rad/sec ($\omega = 66.38$ rad/sec). The tendency of the spin rate to decrease with increasing frequency for a base oscillation amplitude of 2.5 mm also persists.

Figure 8 shows graphs of the average spin rates with their confidence intervals of the experiments for different values of the amplitude and frequency of oscillations of the base. For the above-mentioned ranges of these parameters, the spinning on the base oscillating with an amplitude of 2.5 mm and frequency of 7 Hz turned out to be the most stable (the longest). These values represented the limiting factors for technical realization. Further increase requires developing a new design of the vibrating base. Despite this fact, such approximate methods of experimental estimation have made it possible to observe the stabilization of rotation of the top by means of vibrations of the base.

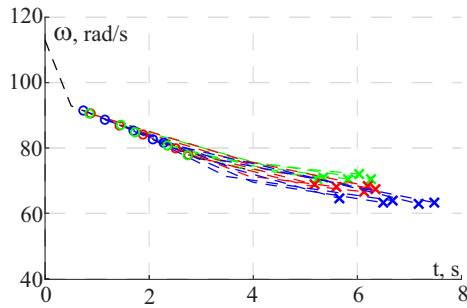


FIGURE 6. The spin rates of the body versus time on a vibrating base with an amplitude of 0.5 mm for different initial spin rates under oscillations of the surface with a frequency of 3 Hz (green), 5 Hz (red), and 7 Hz (blue).

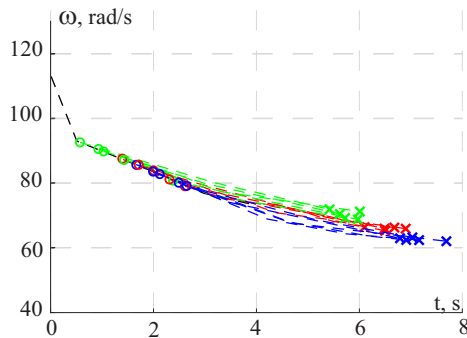


FIGURE 7. The spin rates of the body versus time on a vibrating base with an amplitude of 2.5 mm for different initial spin rates.

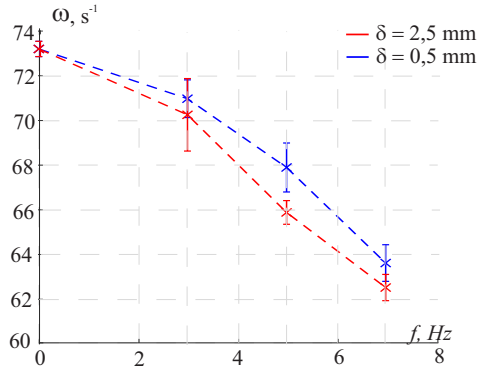


FIGURE 8. The spin rates of the body versus time on a vibrating base for different initial spin rates and surface oscillation parameters

4. Conclusions

The above investigations have made it possible to observe in practice a stabilization of the motion of a spherical top under oscillations of the surface on which it spins. It should be noted that the experiment turned out to be fairly simple and did not require expensive high-precision equipment; therefore, repeating the experiment would not require much effort. Moreover, we have mentioned several questions that warrant more thorough investigations.

In the simulations it was assumed that, with increasing amplitude and frequency of oscillations, there is a decrease in the spin rate at which the top loses stability while spinning in the inverted position, i.e., it continues moving for a longer time. In the model (2.1), the change in the critical spin rate of the top (at which a fall occurs) relative to the critical spin rate without vibrations is a function depending on the product of the frequency and the amplitude of oscillations:

$$\Delta\omega^2 = F(\delta f),$$

where $\Delta\omega^2 = \omega_0^2 - \omega_*^2$.

Figure 9 shows the experimental dependence of $\Delta\omega^2(\delta f)$. As can be seen from the figure, experimental dependences for different amplitudes do not lie on the same curve. This suggests that the dependences of $\Delta\omega^2$ on the oscillation amplitude δ and on the oscillation frequency f are different in nature.

Figure 10 shows separate dependences of $\Delta\omega^2$ on f for the values of the oscillation amplitudes considered in the experiments. These dependences provide evidence of the quadratic dependence of $\Delta\omega^2$ on f . However, the same figure indicates that the dependence of $\Delta\omega^2$ on δ is not quadratic. To determine the experimental dependence of $\Delta\omega^2(\delta, f)$, we approximate it as follows:

$$\Delta\omega^2 = (\alpha + \beta\delta)f^2.$$

Next, we calculate the coefficients α and β from the available experimental data. To do so, we depict the available experimental data on the plane $(\frac{\Delta\omega^2}{f^2}, \delta)$

(see Fig. 11) and approximate them by the straight line $(\frac{\Delta\omega^2}{f^2}) = \alpha + \beta\delta$. As a result, we obtain the following dependence:

$$\Delta\omega^2 = (4140\delta + 28.7)f^2,$$

which is plotted as a solid line in Fig. 11.

The theoretical dependence $\Delta\omega^2 = \kappa^2\delta^2 f^2$, which corresponds to condition (2.1), where $\kappa = 429$ for the parameters of an equivalent ellipsoid, is shown in Fig. 11 as a dashed line.

The significant differences of the theoretical curve on the experimental dependence stem from the fact that the model (2.1) was constructed with the help of averaging theory for the case of “fast” oscillations of the plane. In our case, oscillations of the plane cannot be regarded as fast compared to the typical spin rates of the top. Although in the experiment the quadratic dependence of $\Delta\omega^2$ from

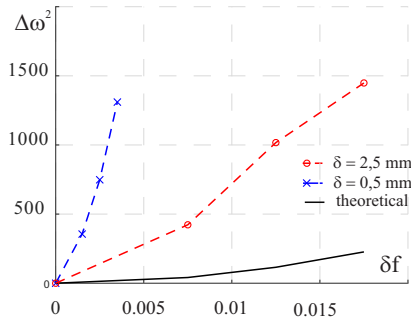


FIGURE 9. The critical spin rate versus the frequency and amplitude of oscillations

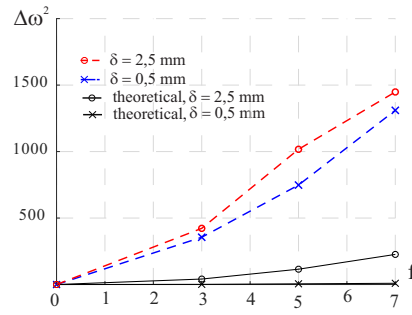


FIGURE 10. The critical spin rate versus the oscillation frequency

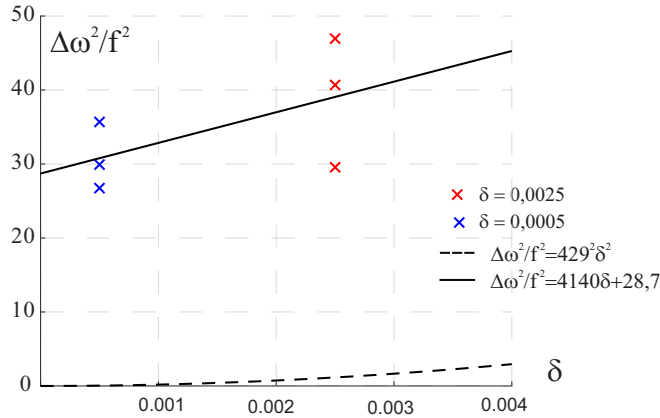


FIGURE 11. Influence of the oscillation amplitude on the change in the spin rate

frequency f persists, the description of its dependence on the oscillation amplitude δ requires developing a new stability criterion using a complete (unaverage) model. This criterion was formulated for a spherical robot on a vibrating base in [20].

The amount of experimental data available only for two values of the oscillation amplitude allows consideration of the dependence of $\Delta\omega^2(\delta)$ only in the linear approximation. However, it is obvious that in the chosen ranges of values the influence of the oscillation amplitude is much smaller than the influence of the frequency. This understanding is of particular importance when it comes to technical implementation, because, in practice, changes in the oscillation frequency over a wide range are easier to achieve than changes in the oscillation amplitude.

For a more detailed study of this dependence in the future, it is planned to widen the ranges of frequency and amplitude of oscillations. This will allow a comprehensive assessment of the applicability of the proposed model. It is also important to carry out research on other specimens of tops (which have different mass-inertia and geometric parameters).

Furthermore, for a better agreement with experimental data, it is necessary to develop a new theoretical model. This effort can be pursued along two avenues: modification of the proposed model by incorporating resistance forces (friction) and representation of the top in a form other than that of an ellipsoid.

These investigations will allow an identification of the top's parameters and vibration parameters for which the stabilization of motion will be observed for a longer time.

Acknowledgments. The authors extend their gratitude to Elena Pivovarova for fruitful discussions. The work of Y. L. Karavaev was carried out within the framework of the state assignment of the Ministry of Education and Science of Russia FZZN-2020-0011. The work of A. Kilin was carried out within the framework of the state assignment of the Ministry of Science and Higher Education of Russia (FEWS-2020-0009).

References

1. C. M. Cohen, *The tippe top revisited*, Am. J. Phys. **45** (1977), 12–17.
2. M. C. Ciocci, B. Malengier, B. Langerock, B. Grimontprez, *Towards a prototype of a spherical tippe top*, J. Appl. Math. **2012** (2012), 268537.
3. R. Cross, *Dynamics of a spherical tippe top*, Eur. J. Phys. **39** (2018), 035001.
4. N. M. Bou-Rabee, J. E. Marsden, L. A. Romero, *Tippe top inversion as a dissipation induced instability*, SIAM J. Appl. Dyn. Syst. **3**(3) (2004), 352–377.
5. A. C. Or, *The dynamics of a tippe top*, SIAM J. Appl. Math **54**(3) (1994), 597–609.
6. D. M. Klimov, V. P. Zhuravlev, *On the dynamics of the thompson top (tippe top) on the plane with real dry friction*, Mech. Solids **40** (2005), 117. (in Russian)
7. A. V. Karapetyan, *Global qualitative analysis of tippe-top dynamics*, Mech. Solids **43** (2008), 33–41. (in Russian)
8. A. A. Zobova, A. V. Karapetyan, *Analysis of the steady motions of the tippe top*, J. Appl. Math. Mech **73** (2009), 623–630. (in Russian)
9. R. Usubamatov, M. Bergander, S. Kapayeva, *The mathematical model for the tippe top inversion*, Adv. Math. Phys. (2021), 5552369.
10. A. A. Kilin, E. N. Pivovarova, *The influence of the first integrals and the rolling resistance model on tippe top inversion*, Nonlinear Dyn. **103** (2021), 419–428.

11. A. V. Borisov, A. A. Kilin, I. S. Mamaev, *How to control Chaplygin's sphere using rotors*, Regul. Chaotic Dyn. **17** (2012), 258–272.
12. Y. L. Karavaev, A. A. Kilin, *Nonholonomic dynamics and control of a spherical robot with an internal omnivheel platform: Theory and experiments*, Proc. Steklov Inst. Math. **295** (2016), 158–167.
13. S. A. Tafriishi, M. Svinin, M. Yamamoto, Y. Hirata, *A geometric motion planning for a spinning sphere on a plane*, Appl. Math. Modelling **121** (2023), 542–561.
14. T. B. Ivanova, Y. L. Karavaev, A. A. Kilin, *Control of a pendulum-actuated spherical robot on a horizontal plane with rolling resistance*, Arch. Appl. Mech. **92** (2022), 137–150.
15. Y. L. Karavaev, *Spherical robots: An up-to-date overview of designs and features*, Russ. J. Nonlinear Dyn., **18** (2022), 699–740.
16. A. Diouf, et al. *Spherical rolling robots—design, modeling, and control: A systematic literature review*, Robot. Auton. Syst. (2024), 104657.
17. A. A. Kilin, E. N. Pivovarova, *Nonintegrability of the problem of a spherical top rolling on a vibrating plane*, Vestn. Udmurt. Univ., Mat. Mekh. Komp'yut. Nauki **30** (2020), 628–644.
18. A. V. Borisov, A. P. Ivanov, *Dynamics of the tippe top on a vibrating base*, Regul. Chaotic Dyn. **25** (2020), 707–715.
19. A. A. Kilin, *Stability of vertical rotations of an axisymmetric ellipsoid on a vibrating plane*, Mathematics **11** (2023), 3948. <https://doi.org/10.3390/math11183948>
20. A. A. Kilin, E. N. Pivovarova, *Stability and stabilization of steady rotations of a spherical robot on a vibrating base*, Regul. Chaotic Dyn. **25** (2020), 729–752
21. A. A. Kilin, E. N. Pivovarova, *A particular integrable case in the nonautonomous problem of a Chaplygin sphere rolling on a vibrating plane*, Regul. Chaotic Dyn. **26** (2021), 775–786.
22. A. A. Kilin, E. N. Pivovarova, *Motion control of the spherical robot rolling on a vibrating plane*, Appl. Math. Modelling **109** (2022), 492–508.
23. A. A. Kilin, T. B. Ivanova, E. N. Pivovarova, *Stabilization of steady rotations of a spherical robot on a vibrating base using feedback*, Regul. Chaotic Dyn. **28** (2023), 888–905.
24. A. Stephenson, *On a new type of dynamical stability*, Mem. Proc. Manch. Lit. Phil. Sci. **52** (1908), 1–10.
25. P. Hirsh, *Das Pendel mit Oszillierendem Aufhaengepunkt*, ZAMM **10** (1930), 41–52.
26. E. L. Ince, *Mathieu functions of stable type*, Phyl. Mag. **6** (1928), 547–558.
27. A. Erdelyi *Ueber die kleinen Schwingungen eines Pendels mit oszillierendem Aufhaengepunkt*, ZAMM **14** (1934), 235–247.
28. P. Kapitza, *A pendulum with oscillating suspension*, Uspekhi Fiz. Nauk **44** (1951), 7–20
29. I. Gutman, *Industrial Uses of Mechanical Vibrations*, Business Books Limited, London, 1968.
30. I. I. Blechman, *Vibrational Mechanics*, Allied Publishers, 2003.
31. H. Takano, *Motion of an articulated straw along a vibrating rod*, Russ. J. Nonlinear Dyn. **20**(4) (2024), 529–551.
32. A. Y. Shamin, A. A. Rachkov, *On the motion of a vibrating robot on a horizontal plane with anisotropic friction*, Russ. J. Nonlinear Dyn. **20**(5) (2024), 945–959.
33. M. V. Belichenko, *On the stability of pendulum-type motions in the approximate problem of dynamics of a lagrange top with a vibrating suspension point*, Russ. J. Nonlinear Dyn. **14** (2018), 243–263.
34. B. S. Bardin, A. A. Savin, *On the orbital stability of pendulum-like oscillations and rotations of a symmetric rigid body with a fixed point*, Regul. Chaotic Dyn. **17** (2012), 243–257.
35. V. I. Yudovich, *Vibrodynamics and vibrogeometry in mechanical systems with constraints*, Uspekhi Mekh. **4** (2006), 26–158. (in Russian)
36. A. P. Markeyev, *The equations of the approximate theory of the motion of a rigid body with a vibrating suspension point*, J. Appl. Math. Mech. **75**(2) (2011), 132–139; see also: Prikl. Mat. Mekh. **75** (2011), 193–203.
37. O. V. Kholostova, *On the periodic motion of Lagrange's top with vibrating suspension*, Mech. Solids **1** (2002), 26–38.

38. O. V. Kholostova, *On a case of periodic motions of the lagrangian top with vibrating fixed point*, Regul. Chaotic Dyn. **4** (1999), 81–93.
39. I. A. Bizyaev, A. V. Borisov, S. P. Kuznetsov, *Chaplygin sleigh with periodically oscillating internal mass*, EPL **119** (2017), 60008.
40. I. A. Bizyaev, A. V. Borisov, I. S. Mamaev, *The Chaplygin sleigh with parametric excitation: Chaotic dynamics and nonholonomic acceleration*, Regul. and Chaotic Dyn. **22** (2017), 955–975.
41. A. V. Borisov, A. A. Kilin, E. N. Pivovarova, *Speedup of the Chaplygin top by means of rotors*, Dokl. Phys. **64** (2019), 120–124.
42. F. L. Chernousko, N. N. Bolotnik, T. Yu. Figurina, *Optimal control of vibrationally excited locomotion systems*, Regul. Chaotic Dyn. **18** (2013), 85–99.
43. F. L. Chernousko, N. N. Bolotnik, *Rectilinear Periodic Motions of Systems with Internal Bodies*, In: Dynamics of Mobile Systems with Controlled Configuration, 255–367, 2024, Springer, Singapore.
44. N. Bolotnik, P. Schorr, et. al., *Periodic locomotion of a two-body crawling system along a straight line on a rough inclined plane*, ZAMM-Z. Angew. Math. Mech. **98** (2018), 1930–1946.
45. N. N. Bolotnik, F. L. Chernousko, et. al., *Regular motion of a tube-crawling robot in a curved tube*, Mechanics of Structures and Machines **30** (2002), 431–462.
46. M. Dosaev, V. Samsonov, Sh.-Sh. Hwang, *Construction of control algorithm in the problem of the planar motion of a friction-powered robot with a flywheel and an eccentric weight*, Appl. Math. Model. **89** (2021), 1517–1527.
47. N. N. Bolotnik, I. M. Zeidis, et. al., *Dynamics of controlled motion of vibration-driven systems*, J. Comput. Syst. Sci. Int. **45** (2006), 834–840.
48. X. Zhan, J. Xu, H. Fang, *Planar locomotion of a vibration-driven system with two internal masses*, Appl. Math. Modelling **40** (2016), 871–885.
49. X. Zhan, J. Xu, H. Fang, *A vibration-driven planar locomotion robot-shell*, Robotica **36** (2018), 1402–1420.
50. A. Sakharov, *Rotation of the body with movable internal masses around the center of mass on a rough plane*, Regul. Chaotic Dyn. **20** (2015), 428–440.
51. A. P. Ivanov, *Vibroimpact mobile robot*, Russ. J. Nonlinear Dyn. **17** (2021), 429–436.
52. J. Awrejcewicz, G. Kudra, *Mathematical modelling and simulation of the bifurcational wobblestone dynamics*, Discontin. Nonlinearity Complex. **3** (2014), 123–132.
53. J. Awrejcewicz, G. Kudra, *Dynamics of a wobblestone lying on vibrating platform modified by magnetic interactions*, Procedia IUTAM **22** (2017), 229–236.
54. F. Chekirou, K. Brahim, et. al., *Analysis of the vibrational behavior of a bolted beam in the presence of friction*, Russ. J. Nonlinear Dyn. **18** (2022), 3–18.
55. V. I. Babitsky, A. Shipilov, *Resonant Robotic Systems*, Springer-Verlag Berlin Heidelberg, 2003.
56. J. P. Baltanás, L. Lopez, et. al., *Experimental evidence, numerics, and theory of vibrational resonance in bistable systems*, Phys. Rev. E **67** (2003), 066119.

ЕКСПЕРИМЕНТАЛНО ПОСМАТРАЊЕ СТАБИЛИЗАЦИЈЕ РОТАЦИЈЕ СФЕРНЕ ЧИГРЕ НА РАВНИ КОЈА ВИБРИРА

РЕИМЕ. Овај рад представља експериментално проучавање кретања сферног тела са помереним центром масе на равни која осцилује у вертикалном правцу. Откривен је феномен вибростабилизације нестабилног положаја у коме је центар масе тела изнад геометријског центра сфере. Анализиран је утицај фреквенције и амплитуде осцилација равни на стабилизацију нестабилног положаја кретања сферног тела.

Ural Mathematical Center
Udmurt State University
Izhevsk
Russia
kilin@rcd.ru
<https://orcid.org/0000-0003-1358-5960>

(Received 04.12.2024)
(Available online 10.01.2025)

Kalashnikov Izhevsk State Technical University
Izhevsk
Russia
karavaev_yury@istu.ru
<https://orcid.org/0000-0002-6679-1293>